Journal of the Neurological Sciences, 122 (1994) 189–203

JNS 4230

Flow rate of cerebrospinal fluid (CSF) – a concept common to normal blood-CSF barrier function and to dysfunction in neurological diseases

Hansotto Reiber *

Neurochemisches Labor, Universität Göttingen, Robert-Koch-Straße 40, D-3400 Göttingen, Germany

(Received 14 October, 1992)
(Revised, received 23 September, 1993)
(Accepted 11 October, 1993)

Key words: Cerebrospinal fluid; CSF flow; Blood CSF barrier; Selectivity; Permeability; Protein diffusion; CSF/serum quotients; Albumin; IgG; IgA; IgM; Neurological diseases; Pathophysiology

Summary

Many neurological diseases are accompanied by increased protein concentrations in the cerebrospinal fluid (CSF), described as a blood-CSF barrier dysfunction. The earlier interpretation as a "leakage" of the blood-CSF barrier for serum proteins could be revised by introduction of a "population variation coefficient" of the CSF/serum quotients for IgG, IgA and IgM ($\Delta Q/\overline{Q}$) which is evaluated as a function of increasing albumin quotients (Q_{Alb}). The data presented here are based on specimens from 4380 neurological patients. These population variation coefficients were found to be constant over two orders of magnitude of normal and pathological CSF protein concentrations ($Q_{Alb} = 1.6 \cdot 10^{-3}$–$150 \cdot 10^{-3}$). This constancy indicates that there was no change in blood-CSF barrier related structures with respect to diffusion controlled protein transfer from blood into CSF and hence no change in molecular size dependent selectivity. The pathological increase of plasma protein concentrations in CSF in neurological diseases could also be explained quantitatively by a decrease of CSF flow rate due to its bifunctional influence on CSF protein concentration: reduced volume exchange, and as newly stated, increased molecular net flux into CSF without change of permeability coefficients. Again, on the basis of a changing CSF flow rate, the hyperbolic functions, which describe empirically the changing quotient ratios between proteins of different size (e.g. $Q_{IgG} : Q_{Alb}$) with increasing CSF protein content (Q_{Alb}) can likewise be derived from the laws of diffusion as the physiologically relevant description. The hyperbolic discrimination line between brain-derived and blood-derived protein fractions in CSF in the quotient diagrams for CSF diagnosis can be further improved on the basis of the large number of cases investigated. Other physiological and pathological aspects, such as high CSF protein values in the normal newborn, in spinal blockade, in meningeal inflammatory processes, CNS leukemia or polyradiculitis as well as animal species dependent variations can each be interpreted as due to a difference or change in the CSF flow rate.

Introduction

Plasma proteins in CSF

Low concentrations of plasma proteins appear in the ventricular cerebrospinal fluid secreted from the choroid plexus. Additionally, plasma proteins enter the CSF on its flow through the subarachnoid space (Frick and Scheid-Seydel 1958; Davson 1967; Cutler et al. 1967) increasing the lumbar protein concentration up to three times that of the ventricular concentration. CSF bulk flow drains the proteins together with cells and other components by passing through the arachnoid villi and granulations into the venous blood (Upton and Weller 1985).

Protein transfer from blood to CSF is a diffusion controlled process, by which the molecular size dependent concentration gradients (Felgenhauer 1974) are established. The gradient is steeper for larger molecules (~ 200:1 for albumin or about 3000:1 for IgM). This retention of proteins is called the blood-CSF barrier. The molecular size dependent difference of protein gradients is defined as selectivity of the barrier function. The steady state concentration of a single plasma protein in CSF depends on the absolute level of the serum concentration, the gradient and the CSF flow rate. CSF/serum or CSF/plasma concentration quotients describe the concentration gradient with increasing values for increasing CSF protein concentra-

* Tel.: +49-551/39 66 19; Fax: +49-551/39 84 05.

SSDI 0022-510X(93)E0241-Z

tion. The quotient is independent of the individual absolute serum concentration level, but reflects all blood-CSF barrier related influences (molecular size, CSF flow, pathlength of diffusion) and conditions of CSF extraction (volume of extraction or locus of extraction, like ventricles or lumbar sac). The albumin CSF/serum concentration quotient has been recognized as a suitable parameter to characterize these individual variables of the blood-CSF barrier function and has been introduced as a suitable reference for the most sensitive evaluation of other plasma proteins in CSF, due to the reduction of individual variables (Reiber 1980). Many approaches for the discrimination of a brain-derived, pathological IgG fraction from a blood-derived IgG fraction in CSF have been reported (Ref. in Thompson 1988). Linear discrimination lines (Link and Tibbling 1977; Tourtellotte and Ma 1978), bifunctional lines (Reiber 1980), or nonlinear approaches (Reiber and Felgenhauer 1987; Thompson 1988; Öhman et al. 1992) have been reported. The hyperbolic function (Reiber and Felgenhauer 1987) has been shown empirically to be a best fit for the clinical data (Souverijn et al. 1991; Öhman et al. 1992). The application of Fick's laws of diffusion for protein transfer from blood to CSF now gives theoretical support for the hyperbolic function, as the physiologically exact description of the changing ratio between two CSF/serum quotients ($Q_{IgG} : Q_{Alb}$) with increasing protein content in CSF.

Pathophysiology

Many neurological diseases have a concomitant increase of plasma protein concentrations in CSF. Under these circumstances the quotient values of different sized proteins (Q_{IgG}, Q_{Alb}) approach to each other. This was interpreted as a decline of selectivity with increased permeability, due to a blood-CSF barrier "impairment", "dysfunction" or "leakage". There have been many contradictions to such a hypothesis which have been ignored.

A diffusion related increase of CSF concentration for solutes from blood without a change in barrier structures was recognized as early as 1925 by Cestan et al., as interpreted by Davson (1967). Additionally, the flow rate of cerebrospinal fluid has been known for more than 40 years to influence the concentrations of proteins in CSF, as previously reviewed by Davson (1967).

These approaches, which involved both aspects, diffusion and CSF flow into a model (Rapoport 1983), still suffered from the postulated loss of selectivity and increase of the barrier permeability. The introduction of the population variation coefficient for immunoglobulin quotients offers the empirical basis to show that there is no loss of selectivity in blood-CSF barrier dysfunction.

Population variation coefficient

This term defines the biological variation of a parameter in a group large enough to be labelled as population. Since clinical chemists use the term coefficient of variation to characterize the variation due to methodological imprecision, so the expression population variation coefficient has been chosen to reinforce the special meaning as a natural variation in a biological group. In this paper it refers to the variation of immunoglobulin quotients in persons or patients with the same albumin quotient. If this population variation coefficient does not depend on cause or intensity of neurological diseases, the relevant structures for the CSF/serum concentration gradients should not be changed by the diseases. This constancy, reported in this paper with the application of the laws of diffusion has led to a new description of the physiology of the blood-CSF barrier function as well as for understanding of the pathophysiology of the blood-CSF barrier dysfunction: A reduced CSF flow rate induces increased protein concentrations in CSF due to decreased volume exchange and is followed by a subsequent change in blood-CSF concentration gradients with an initially increasing molecular net flux of proteins into CSF without changes in blood-CSF barrier related structures. This mechanism is relevant for normal as well as for pathological variations of CSF flow rate.

These aspects have been applied to several aspects of physiology and pathophysiology of CSF and subarachnoidal space with surprising results for consistent interpretations.

Materials and methods

Patients

The data from lumbar CSF and serum from controls and patients with various neurological diseases (ages between 0.5 and 75 years) were collected from patients routinely diagnosed over the last eight years at the Neurological Clinic, University Göttingen. Only subjects who had no antibody synthesis in the central nervous system were included in the study, using the following criteria: no oligoclonal IgG in CSF (detectable by isoelectric focusing on polyacrylamid gels); no local IgA or IgM synthesis according to the quotient diagrams (Reiber and Felgenhauer 1987) and in each case $Q_{IgA} < Q_{IgG}$ and $Q_{IgM} < Q_{IgA}$; no intracerebral haemorrhage, no blood contamination at all; no patients after neurosurgery or head trauma; cell count

$< 4/\mu l$ for cases $Q_{Alb} < 8 \cdot 10^{-3}$. The statistical evaluation was performed on only those cases in which all four quotients (Alb, IgG, IgA, IgM) have been available.

Protein analysis

Albumin and IgG were measured by automated immunochemical nephelometry (Reiber and Felgenhauer 1987). IgA and IgM were measured by an enzyme immunoassay with a sensitivity of 0.05 mg/l. The day-to-day coefficient of variation for CSF/serum quotients were CV $< 5\%$ (Q_{Alb}, Q_{IgG}) and CV $< 8\%$ (Q_{IgA}, Q_{IgM}).

Curve fit and calculations

For calculation of the mean CSF/serum quotients of immunoglobulins (IgG, IgA, IgM) 30–70 cases with similar albumin quotients were grouped together (as shown in the Figs. 1–3 with Q_{Alb} intervals from $0.1 \cdot 10^{-3}$ to $1.0 \cdot 10^{-3}$ or larger intervals for albumin quotients between $21 \cdot 10^{-3}$ and $150 \cdot 10^{-3}$ with groups of at least ten cases. The upper and lower border curves (envelope curves) as well as the mean were fitted by a hyperbolic function, according to the procedure reported (Reiber and Felgenhauer 1987) with the equation

$$Q_{IgX} = a/b \sqrt{Q_{Alb}^2 + b^2} - c$$

The upper and lower curves were fitted so as to involve 99% of the cases, corresponding to a range of ± 3 SD (standard deviations) in the case of a Gaussian distribution.

Population variation coefficient

The population variation coefficient ($\Delta Q/\overline{Q}$) for the immunoglobulin CSF/serum quotients is defined according to Fig. 4. For example: patients with an albumin quotient of $Q_{Alb} = 25 \cdot 10^{-3}$ might have an IgG quotient Q_{IgG} between 8.0 and $21.6 \cdot 10^{-3}$. This range describes the difference between upper and lower border line. From $\Delta Q_{IgG} = 13.6 \cdot 10^{-3}$ with the mean $\overline{Q}_{IgG} = 15 \cdot 10^{-3}$ the coefficient of variation can be calculated as $\Delta Q_{IgG}/\overline{Q}_{IgG} = 13.6/15 = 0.91$ for the whole population with $Q_{Alb} = 25 \cdot 10^{-3}$. The population variation coefficients for different albumin quotients (Table 2) were calculated from the hyperbolic functions determined for upper and lower border lines and the mean as given in Table 1 and Fig. 3.

TABLE 1

PARAMETER VALUES OF THE HYPERBOLIC FUNCTIONS ($Q_{IgX} = a/b \sqrt{Q_{Alb}^2 + b^2} - c$) IN QUOTIENT DIAGRAMS FOR IgG, IgA AND IgM CSF/SERUM QUOTIENTS AS A FUNCTION OF THE ALBUMIN QUOTIENT, Q_{Alb}

IgX		a/b	b^2	c
IgG	upper limit	0.93	6	1.7
	mean	0.65	8	1.4
	lower limit	0.33	2.0	0.3
IgA	upper limit	0.77	23	3.1
	mean	0.47	27	2.1
	lower limit	0.17	74	1.3
IgM	upper limit	0.67	120	7.1
	mean	0.33	306	5.7
	lower limit	0.04	442	0.82

Results

The CSF/serum concentration quotients of IgG, IgA and IgM are shown as a function of the corresponding albumin quotient for controls or patients with neurological diseases without an intrathecal immunoglobulin synthesis at the time of investigation.

Fig. 1 represents the data of 4154 cases with normal or moderately increased albumin quotients up to $Q_{Alb} = 21 \cdot 10^{-3}$. In Fig. 2 the data of patients (n = 226) with severely increased CSF protein content with albumin quotients up to $Q_{Alb} = 150 \cdot 10^{-3}$ are shown. For increasing intervals with similar albumin quotients the mean values of the IgG, IgA and IgM quotients have been calculated (Fig. 3). For the complete set of data in Figs. 1 and 2 the upper and lower border lines and the lines for the mean values (Fig. 3) were fitted by

TABLE 2

POPULATION VARIATION COEFFICIENTS, $\Delta Q/\overline{Q}$, AS A FUNCTION OF INCREASING PROTEIN CONCENTRATION IN CSF, I.E. INCREASING ALBUMIN CSF/SERUM CONCENTRATION QUOTIENT, Q_{Alb}

$Q_{Alb} \cdot 10^3$	$\Delta Q/\overline{Q}$		
	IgG	IgA	IgM
2.2	0.86	1.36	3.0
3.5	0.89	1.41	3.0
5.0	0.90	1.43	3.1
8.2	0.92	1.42	2.9
10.0	0.91	1.40	2.9
15	0.91	1.38	2.7
20	0.91	1.34	2.6
50	0.92	1.31	2.2
100	0.92	1.29	2.0
140	0.92	1.29	2.0
Mean	0.91 ± 0.01	$1.35 + 0.06$	2.0(lim) *

* Limit value, due to non-Gaussian distribution around mean for small "Q_{Alb}".

hyperbolic functions as described in the methods and legend to Fig. 1. Table 1 gives the constants of the single hyperbolic functions for the IgG, IgA and IgM diagrams. The mean curve is almost identical with the arithmetic mean of upper and lower curve except for the range of low albumin quotients in the IgM-diagram. This discrepancy is the consequence of a non-gaussian distribution in this range of extremely low CSF IgM values.

In Fig. 2 the corresponding data of three representative patients (Reiber 1993) have been marked in all three diagrams. Patient 1 with data at the upper border lines of the reference ranges has larger IgG, IgA and IgM quotients than patient 3 in spite of a similar albumin quotient, which can be interpreted as having a weaker molecular size dependent discrimination between larger and smaller molecules than patient 3. These three patients with the same type of disease (early phase of bacterial meningitis), covering the whole range of biological variation between upper and lower border lines, are representative of other groups of neurological diseases involved in this study (Guillain Barré polyradiculitis, meningeal carcinomatosis or spinal blockade) insofar as the statistical evaluation of the quotient data for these diseases did not allow a significant discrimination with respect to localization in the diagram (restricted to upper, mean or lower range). Even for cases with extremely high protein concentrations ($Q_{Alb} > 150 \cdot 10^{-3} = 0.15$) there is a complete overlap of the values from patients with different neurological diseases (Reiber 1993) as indicated by the following 6 examples (the quotients $Q_{Alb}/Q_{IgG}/Q_{IgA}/Q_{IgM}$ are shown in parentheses): spinal tumor (0.17/0.09/0.067/0.015); meningitis (0.21/0.16/0.11/0.08); ependymoma (0.30/0.24/0.19/0.13); spinal cyst (0.34/0.18/0.10/0.026); paraproteinemia (0.61/0.56/0.50/0.29); meningitis (0.73/0.65/0.47/0.35).

These correlated variations for single patients 1–3 in Fig. 2 as well as the coincident variation of the mean values for IgG, IgA and IgM quotients in Fig. 3 help to understand that the variation of patient values between upper and lower border lines mainly represent biological variations in a group of patients with the same albumin quotient. As these groups are large enough in this investigation to represent a population, it is possible to introduce the population variation coefficient as described in Fig. 4. These population variation coefficients $\Delta Q/\bar{Q}$ have been calculated with the parame-

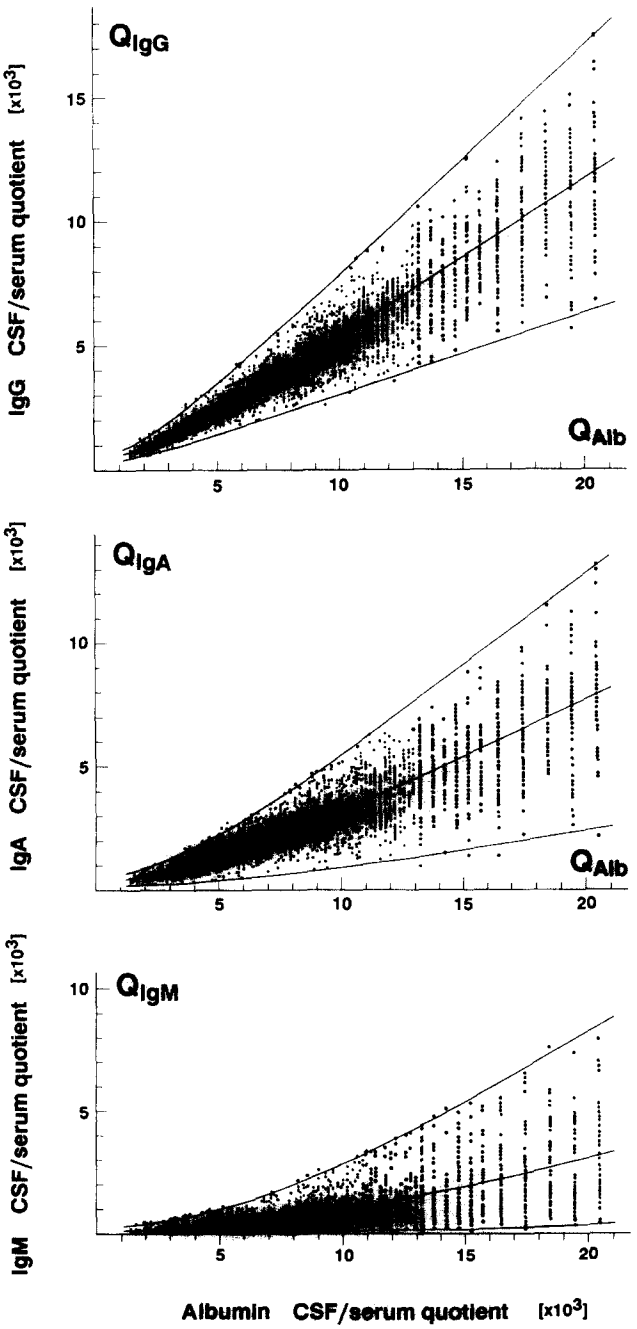

Fig. 1. CSF/serum quotients for IgG, IgA, IgM (Q_{IgG}, Q_{IgA}, Q_{IgM}) as a function of the albumin CSF/serum quotient (Q_{Alb}). The data were calculated for lumbar CSF and serum from 4154 control patients and patients with various neurological diseases (with albumin quotients below $Q_{Alb} = 21 \cdot 10^{-3}$). Albumin and IgG were measured as described (Reiber and Felgenhauer 1987). IgA and IgM were measured by an enzyme immunoassay with a sensitivity of 0.05 mg/l. The day-to-day imprecisions, calculated as coefficients of variation were < 5% (Q_{Alb}, Q_{IgG}) and < 8% (Q_{IgA}, Q_{IgM}). Only cases were included which had no humoral immune response in the central nervous system, according to the criteria in methods. For calculation of the mean values, 30–70 cases with similar albumin quotients were grouped together (as shown in the figure with Q_{Alb} intervals between $0.1 \cdot 10^{-3}$ and $1.0 \cdot 10^{-3}$). The upper and lower border curves, including 99% of the cases, were fitted by hyperbolic functions together with the data from Fig. 2 according to the procedure reported (Reiber and Felgenhauer 1987) with equation $Q_{IgX} = a/b\sqrt{Q_{Alb}^2 + b^2} - c$. The mean curve originates from the procedure shown in Fig. 3. The numerical results are given in Table 1.

ters in Table 1 for varying albumin quotients. The most important result of this evaluation shown in Table 2, was that the population variation coefficients were found to remain constant between the normal albumin

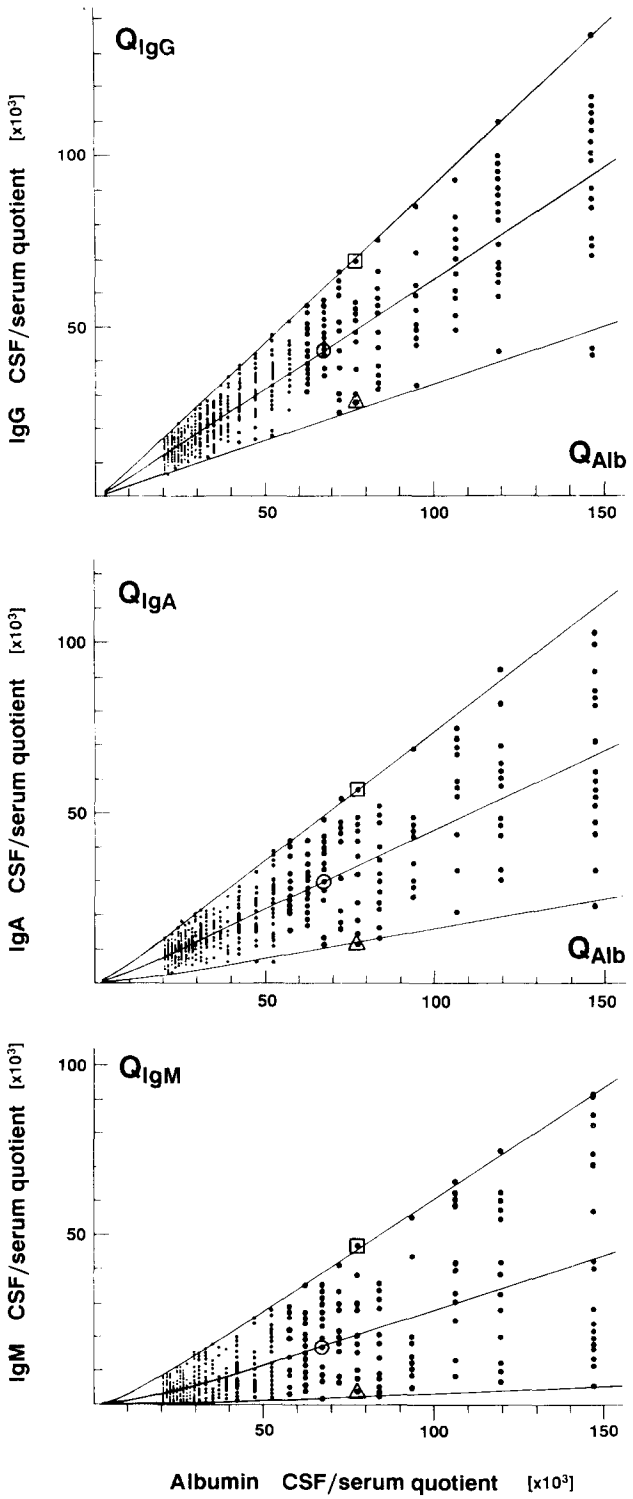

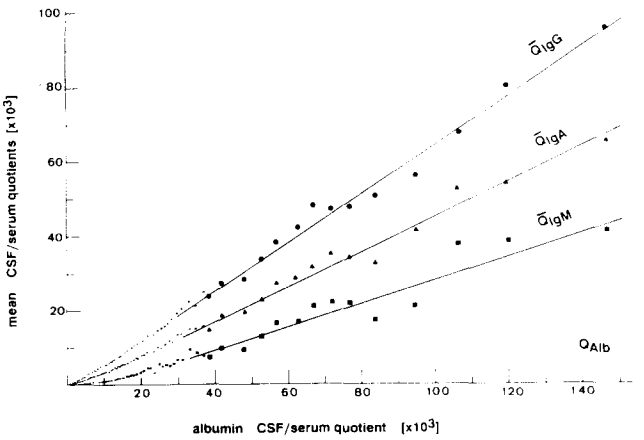

Fig. 3. Mean immunoglobulin quotients Q_{IgG}, Q_{IgA}, Q_{IgM} as a function of an increasing albumin CSF/serum concentration quotient Q_{Alb}. The mean values are calculated from groups of cases (populations) with similar albumin quotients of varying Q_{Alb} intervals, according to the description in Fig. 1 and Fig. 2. The mean values were fitted with a hyperbolic function according to the reported procedure (Reiber and Felgenhauer 1987).

quotients and the most severe blood-CSF barrier dysfunctions (from $Q_{Alb} = 1.6 \cdot 10^{-3}$ to $Q_{Alb} = 150 \cdot 10^{-3}$):

$$\Delta Q_{IgG}/\bar{Q}_{IgG} = 0.91; \quad \Delta Q_{IgA}/\bar{Q}_{IgA} = 1.35;$$

$$\Delta Q_{IgM}/\bar{Q}_{IgM} = 2.0$$

These population variation coefficients for molecules of different size like IgG, IgA and IgM do not approach each other, indicating unchanged conditions for the diffusion controlled protein transfer from blood to CSF. As a striking consequence, this constancy of the population variation coefficients could only be explained in terms of constant blood-CSF barrier structures in spite of hundred-fold increased CSF protein concentrations. A facilitation of protein transfer between blood and CSF based on disturbed barrier structures (e.g. due to leakage) would physically mean a reduction of the effective diffusion path length (Fig. 5) and a subsequent reduction of variation coefficients

Fig. 2. CSF/serum protein concentration quotients from patients with the most severe blood-CSF barrier dysfunction. n = 266 patients, with albumin quotients between $20 \cdot 10^{-3}$ and $150 \cdot 10^{-3}$, fulfilled the criteria reported in legend of Fig. 1. The cases included the following disorders: early meningitis, herniated disc prolapse, polyradiculitis, paraproteinemia, dysgerminoma, ependymoma, meningioma, diabetes mellitus and other disorders. Means were calculated from groups of at least 10 patients with similar albumin quotients between the intervals shown in the diagram. The hyperbolic functions of the upper and lower border lines and the mean curve are fitted together with the data in Fig. 1. The indicated patients 1 (□) 2 (○) and 3 (△) had bacterial meningitis and were punctured for CSF early after onset of clinical symptoms at a time before onset of any humoral immune response.

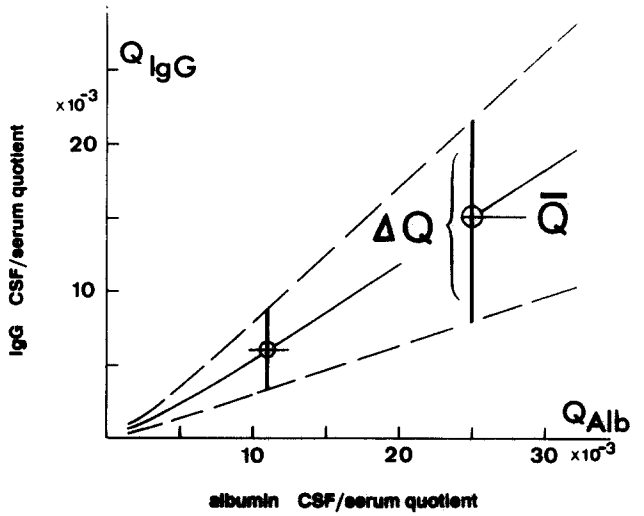

Fig. 4. Definition of the population variation coefficient ($\Delta Q/\bar{Q}$) for the immunoglobulin CSF/serum quotients. For example patients with an albumin quotient of $Q_{Alb} = 25 \cdot 10^{-3}$ might have an IgG quotient Q_{IgG} between 8.0 and $21.6 \cdot 10^{-3}$. This range describes the difference between upper and lower border line involving 99% of the cases by analogy to the mean ± 3 standard deviations in case of a Gaussian distribution: $\Delta Q_{IgG} = 6SD = 13.6 \cdot 10^{-3}$ with $\bar{Q}_{IgG} = 15 \cdot 10^{-3}$. The coefficient of variation for the particular population can be calculated as $\Delta Q_{IgG} / \bar{Q}_{IgG} = 13.6/15 = 0.91$. Population variation coefficients for different albumin quotients in Table 2 were calculated from data of the hyperbolic functions for upper and lower border lines and for the mean given in Table 1.

with increasing albumin quotients. This would be in contradiction to the results above. As shown in Table 3 the variation coefficients for CSF/serum quotients ($\Delta Q/\bar{Q}$) and the corresponding variation coefficients for serum concentrations (6 SD/$\bar{x}$) in the same group of 4380 patients, each remain independent of the other. Both groups of evaluation refer to 99% or ± 3 SD of the population.

Table 4 represents kinetic data from a very early, first lumbar puncture and a later repeated puncture of the same patient with bacterial meningitis. By this kinetic approach – a type of natural "stopped flow" experiment – it is shown that there are larger relaxation times for the protein molecules of larger size to

TABLE 3

COMPARISON OF POPULATION VARIATION COEFFICIENTS FOR CSF/SERUM CONCENTRATION QUOTIENTS ($\Delta Q/\bar{Q}$) AND SERUM CONCENTRATIONS (6 SD/$\bar{x}$) * IN THE SAME GROUP OF PATIENTS ($n = 4400$) EVALUATED IN FIGS. 1–3

		IgG	IgA	IgM
CSF	($\Delta Q/\bar{Q}$)	0.91	1.35	2.0
Blood	(6SD/$\bar{x}$) *	1.8	3.3	3.5

* 6 SD/$\bar{x}$ means 6 standard deviations (SD) divided by the mean of the population (x) which corresponds to the definition of the population variation coefficient including 99% of the population.

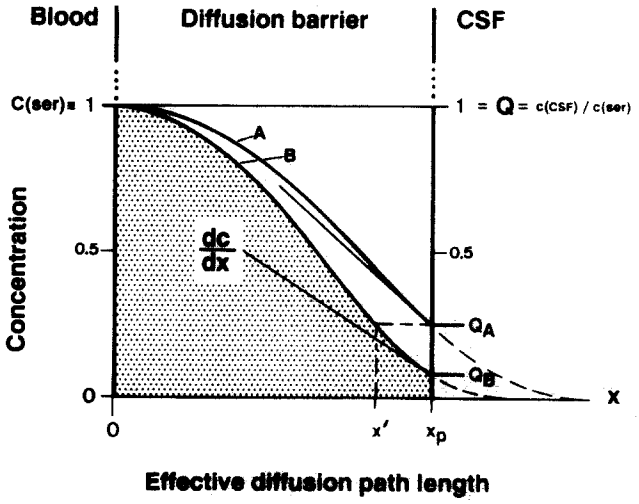

Fig. 5. Protein concentration gradient between blood and CSF. The diffusion controlled protein transfer between blood and CSF is described by an idealized diffusion barrier (homogeneous and unique instead of multistructural, inhomogeneous). The concentration c_i (in blood as c(ser) and in CSF as $Q = c(CSF)/c(ser)$, normalized for $c(ser) = 1$) along the effective diffusion pathlength, x, (x_p, for the single patient), shows the sigmoidal curve, derived from Fick's second law of diffusion (Appendix). At constant t (steady state), the local concentration gradient dc_i/dx determines the molecular flux, J_i, of molecules i into CSF according to Fick's first law of diffusion: $J_i = -D_i\, dc_i/dx$, with D_i, the molecular size- and tissue-dependent diffusion coefficient. J_i or $dc_i/dx(x_p)$ depends on $c_{x,t}$ at x_p or c_{CSF} for the molecules i. The change of (dc_i/dx) along the idealized diffusion pathlength x, follows a Gaussian error curve (Fig. 6) with a maximum for $Q = 0.5$, i.e. half serum concentration. The diagram is used for two different interpretations. Case one: normal steady state condition, where the curves A and B can be interpreted as if they were from molecules of different size (A = albumin and B = IgG) due to different diffusion coefficients. The smaller molecule albumin with the larger diffusion coefficient D_{Alb} reaches a higher tissue concentration (curve A) than IgG (curve B) and therefore a larger local concentration gradient dc/dx at x_p, represented by the slope of the tangential line at x_p. Individual variations of the steady state value of Q_A or Q_B would be a consequence of variations in x_p and in CSF flow rate, r. The function $Q_B = f(Q_A)$ can be shown to be a hyperbolic function (Appendix). The curves A and B with the same function (Eqn. 4, Appendix) differ only in their mean molecular displacement ($x_i = \sqrt{2D_i t}$). In this case for constant t the different diffusion coefficients D_A, D_B, are responsible for the difference. Q_A on curve A at x_p corresponds with the same concentration on curve B at $x' = x_p \cdot (D_B/D_A)^{1/2}$ (Appendix). Case two: now the curves A and B represent the concentration distribution of the same protein (e.g. IgG) at different times, before (t_o, curve B) and after (t_1, curve A) onset of a disease with decreasing CSF flow and subsequently increasing concentration of IgG in CSF. With a secondary increasing tissue concentration, c_{IgG} (x, t), the gradient $(dc_{IgG}/dx)_{x,t}$ increases with t (const x) as shown in Fig. 6 and, as a consequence, the molecular flux, J_{IgG}, is increased as well. This statement is true for cases of $Q_{IgG} < 0.5$ only (normal Q_{IgG}-values are between 0.0005 and 0.005!). Above $Q > 0.5$ (Fig. 6), the gradient (dc_i/dx) is reduced with a subsequently reducing flux of proteins into CSF. In this case the change from curve B to curve A can be explained as an increased mean displacement $x_i = \sqrt{2D_i t}$, where D_i remains constant but t increases.

TABLE 4

KINETICS OF CSF/SERUM CONCENTRATION QUOTIENTS AFTER ONSET OF DISEASE

A patient with bacterial meningitis was punctured on the 1st day and 2nd day after the onset of clinical symptoms. Both punctures were done before onset of a local IgG, IgA or IgM synthesis (no oligoclonal IgG fractions from brain detectable). The increasing cell count in CSF is not the source of a local immunoglobulin synthesis.

	QAlb ($\cdot 10^3$)	QIgG ($\cdot 10^3$)	QIgA ($\cdot 10^3$)	QIgM ($\cdot 10^3$)	cell count
1st day	146	42	22	5	872/μl
2nd day	311	203	184	105	154000/μl

reach the new steady state concentration in CSF. At the first puncture, the albumin CSF concentration reached 47% of the value for day two, compared to 21%, 12% or only 5% for IgG, IgA and IgM values respectively. The smaller molecule albumin appeared 2 times, 4 times or 10 times faster in lumbar CSF than the larger molecules IgG, IgA or IgM. This again is a strong argument for the conservation of blood-CSF barrier "structures" relevant for protein diffusion from blood to CSF in spite of marked blood-CSF barrier "dysfunction".

Discussion and conclusions

Diffusion of proteins into CSF

There is no controversy about the protein transfer from blood to CSF as a diffusion controlled molecular size dependent process (Felgenhauer 1974; Rapoport 1983; and references cited in Davson et al. 1987). In

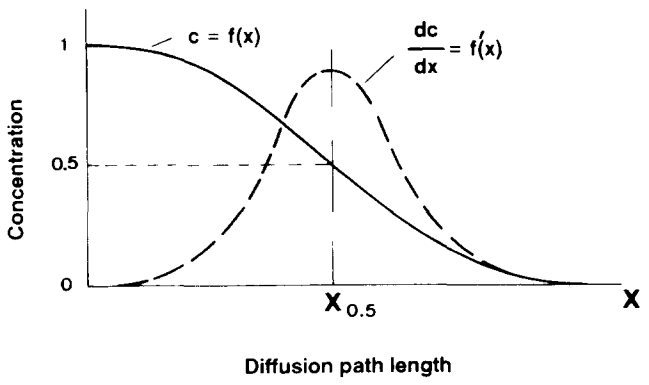

Fig. 6. Curves for the diffusion dependent concentration distribution $c_{x,t}$ (Eqn. 4) and the first derivative $dc/dx = f'(x)$. This derivative represents a Gaussian error curve (Eqn. 3 in Appendix, not to be confused with the error function or error integral obtained by integration of the exponential (Jost 1960, p. 17)). The maximal slope of the error function curve is obtained for $Q = c/c_0 = 0.5$ at $x_{0.5}$. The position $x_{0.5}$ is characterized by the mean molecular displacement $x_i = \sqrt{2 D_i t}$.

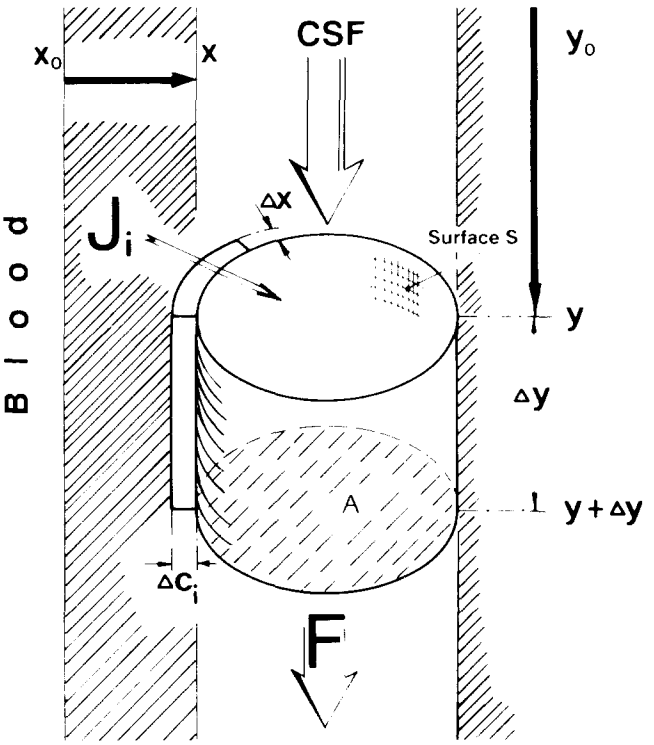

Fig. 7. Model for CSF volume flow (F) through subarachnoid space (y-direction) and molecular flux (J_i) into CSF (x-direction). Cross section area A and surfaces S of the interval Δy in subarachnoid space are idealized. $\Delta c_i/\Delta x$ represents the concentration gradient of a molecule i at surface S. The bulk volume flow $F = \Delta Vol/\Delta t$ (dimension ml/s) characterizes the volume $\Delta Vol = A \cdot \Delta y$ which passes the cross section area A in the time interval Δt. The flow rate of a single molecule in this CSF volume is $r = \Delta y/\Delta t$ (dimension cm/s) or $r = F/A$.

Fig. 5 and Fig. 6 the direction of molecular flux is given as x-axis (x_0 to x in Fig. 7).

In Fig. 5 the protein concentration gradients between blood ($x = 0$) and CSF ($x = x_p$) are described schematically for idealized conditions. The nonlinear function between concentration and diffusion pathlength is described by Fick's laws of diffusion (Appendix). The steady state conditions of molecular flux (case 1 of Fig. 5) are described by $J_i = -D_i\, dc_i/dx$, Fick's first law of diffusion.

The concentration gradient dc/dx depends on the distance x_p from blood and from actual CSF concentration (quotient Q) influenced by the CSF flow rate. dc/dx as a function of x is characterized by a gaussian error curve with a maximum for $c_{ser}/2 = c_0/2$ or $Q = c_{CSF}/c_{ser} = 0.5$ (Fig. 6).

Case one in Fig. 5 shows that this nonlinear concentration gradient is different for molecules of different size (due to different diffusion constants, D_i). The larger molecule IgG (curve B in Fig. 5) has a smaller local gradient dc/dx than the smaller molecule albumin (A in Fig. 5) at the distance x_p from blood. If the

CSF flow decreases with a subsequent increase of Q, the value of dc/dx changes with time:

$$dc/dt = -dJ/dx = D \cdot d^2 c/dx^2.$$

This is explained as case 2 in Fig. 5, where IgG at time t_0 (curve B) changes to IgG concentration at time t_1 (curve A). Initially, dc/dx is increased (in spite of a decreasing concentration difference between blood and CSF), but only up to a value of $Q = 0.5$. Above this value dc/dx decreases with time up to a new steady state (mostly not reached in neurological diseases due to therapy or other interventions). This time dependent change of $(dc/dx)_{x,t}$ is described by Fick's second law of diffusion (Appendix, Eqn. 2) from which we can calculate the influence of diffusion pathlength and time of diffusion on the actual concentration $c_{x,t}$ of a single molecule, influencing the molecular flux, dJ_i/dx, at the surface to subarachnoid space (Eqn. 4, Appendix).

Population variation coefficient

The ratio of two CSF/serum quotients (Q_{IgG}:Q_{Alb}) represents the ratio of the molecular fluxes into CSF, J_{IgG}:J_{Alb}. This ratio changes with increasing protein content in CSF, i.e. an increasing albumin CSF/serum quotient, in a nonlinear way. From diffusion equations it is derived as a hyperbolic function (Appendix). Due to a constant x_p (Fig. 5) and the same CSF flow rate for both molecules in the single patient, the origin of a different molecular flux and different tissue concentration of IgG and albumin remains the diffusion coefficient D_i influencing the ratio of the individual quotients Q_{IgG}, Q_{Alb} in a single patient. The biological variation ΔQ_{IgG} (Figs. 1 and 2, and particular patients 1–3 in Fig. 2) in a certain population with the same Q_{Alb} value is caused by variations of the individual x_p-values and individual CSF flow rates, more likely than by a several fold difference in diffusion constant, D_i, of the single molecule. Thus, the population variation coefficient $\Delta Q/\bar{Q}$ referring to the same Q_{Alb} of this population represents a measure for the molecular size dependent diffusion processes of the whole population of possible x_p-values (Fig. 5) but for a restricted range of CSF flow rates. An increasing Q_{Alb} value is then due to a decreased mean of the range of CSF flow rates in populations with a (per definition) unchanged distribution of x_p-values.

As an alternative interpretation of increasing Q_{Alb} one could suggest a decreasing effective diffusion pathlength. But, in a hypothetical population of patients with smaller x_p values the increased mean concentration $\bar{Q}$ (Fig. 5) would be concomitant with a relatively reduced variation ΔQ. This would mean a decreasing population variation coefficient $\Delta Q/\bar{Q}$ with increasing mean $\bar{Q}$, which is not the case. This phenomenon is an analogy to band broadening in column chromatography with increasing pathlength or time of diffusion.

The observed constancy of the population variation coefficients in our biological system (Table 2) speaks against a change in (mean) effective diffusion pathlength in case of a so-called blood-CSF barrier dysfunction. This is the main argument against a facilitated transfer of proteins from blood to CSF by a type of "leakage" of barrier structures as this would mean a reduction of the effective diffusion pathlength or a reduced time of diffusion. The constant selectivity (see below) and the observed molecular size dependent relaxation of protein transfer from blood to CSF in examples of most severe blood-CSF barrier dysfunction (Table 4; Reiber 1993) are further strong arguments.

The introduction of this population variation coefficient as an indicator for diffusion related changes of the blood-CSF barrier was possible only for the case that there are no disease dependent differences in these variation coefficients. The subjects, selected for this study, satisfy this condition, as seen from a separate statistical evaluation of single groups of different neurological diseases. The observed slight variations between mean quotient ratios of patient groups with various diseases must be interpreted as a longitudinal sampling effect. As the quotient values depend on the time of puncture during the course of the disease (late steady state in tumours or pre-steady state in acute diseases in Table 4) it is important to see representative examples, such as patients 1–3 in Fig. 2, covering the whole range of quotients or the 6 cases described above together with cases described elsewhere (Reiber 1993).

CSF flow rate

The steady state between molecular flux into CSF (J_i) and CSF flow rate (r) determines the CSF concentration of a single protein (Fig. 7 and Appendix). The decrease of CSF flow with a decreasing CSF volume exchange must lead to an increased CSF protein concentration (in spite of a primarily unchanged molecular flux, J_i). So far there is a consensus with the earlier reports (Rapoport 1983). As a new concept, I introduce the statement that the molecular flux, proportional to dc/dx in Fig. 5, increases with increasing CSF protein concentrations as well: an increased CSF protein concentration must lead to an increased tissue protein concentration according to Eq. (13) in Appendix. I refer to $dc/dt = -dJ/dx = D\, d^2c/dx^2$ instead of $J = -Ddc/dx$, i.e. Fick's second law of diffusion is applied instead of Fick's first law. This postulate is concordant with the described sink effect of CSF flow rate on solute concentrations in the extracellular space (Davson 1967; Davson et al. 1987). With increasing c_{CSF}

and subsequently increasing $c_{x,t}$ (Eqn. 13, Appendix), we obtain an increased gradient dc/dx ($c_{CSF} < c_{ser}/2$). This is described as case two in Fig. 5: the steady state concentration gradient of IgG (curve B) changes to that of curve A, now representative for IgG under pathological conditions (reduced CSF flow rate).

As a consequence of this twofold influence of CSF flow rate the actual CSF protein concentration depends nonlinearly on the CSF flow rate (Appendix). This nonlinear relation between CSF flow rate and CSF protein concentration describes quantitatively the increase in CSF protein content. In the Appendix we get a relation $\Delta c(CSF) \sim 1/r^2$, if restricted to $c(CSF) < c_0/2$. If we rearrange this function and insert for c(CSF) the concentration quotient, we get for the change of CSF flow rate as an approximation $\Delta r \sim 1/\sqrt{\Delta Q_{Alb}}$. This function was applied successfully for a clinical example of blood-CSF barrier dysfunction (Reiber et al. 1993).

Permeability and selectivity

The permeability coefficient (usually defined as $P_i = D_i/x$) for protein transfer across the barrier remains constant as long as x, the diffusion pathlength, and D_i, the diffusion coefficient remain constant. The observed nonlinearly increased net molecular flux into the CSF is quantitatively explained by increased brain tissue protein concentration (case 2 in Fig. 5 and Appendix), without any change in the permeability coefficient. The faster protein transfer from blood to CSF in case of a blood-CSF barrier dysfunction needs no structural change or increased "permeability". This increased brain tissue protein concentration can be described as an increased mean molecular displacement ($\bar{x} = \sqrt{2D_i t}$), as defined in Appendix and shown as $\bar{x} = x_{0.5}$ in Fig. 6.

The changing ratio between different protein species with increasing total protein content in CSF still remains to be discussed. The mean ratio of $\overline{Q}_{IgM} : Q_{Alb} = 1:17$ at $Q_{Alb} = 4.6 \cdot 10^{-3}$ changes to $\overline{Q}_{IgM} : Q_{Alb} = 1:3.6$ at $Q_{Alb} = 100 \cdot 10^{-3}$ (calculated from Table 1). This declining ratio was erroneously interpreted as loss of selectivity.

As derived from Fick's laws of diffusion in the Appendix, the hyperbolic function is the relevant description of the changing ratio of the two quotients, only depending on the ratio between the square root of diffusion coefficients $(D_B : D_A)^{1/2}$.

The kinetic data in Table 4 indicate that in spite of marked blood-CSF barrier dysfunction ($Q_{Alb} = 0.1$–0.3!) the molecular size dependent relaxation time between influx of IgG and albumin into CSF corresponds to the delay in equilibration time between plasma and CSF reported for normal blood-CSF barrier functions (Frick and Scheid-Seydel 1958; Cutler et al. 1967).

As shown in Table 4 or by the above examples of the most severe blood-CSF barrier dysfunctions, there are no cases reported where the Q_{Alb} values reach the theoretical maximum of 1 or where the Q_{IgM} values (0.3) approach the Q_{Alb} values (0.7) completely. Together with the non-negligible reflux rate in Eq. (7) (Appendix), under conditions with $Q > 0.5$ where dc/dx decreases (Figs. 5 and 6), these limitations in steady state of severe dysfunctions can be explained.

If selectivity is defined as the molecular size-dependent discrimination for protein transfer from blood into CSF, depending on the ratio of diffusion constants of the single molecules then there is no reason to postulate a change in selectivity. The actual concentration ratios between molecules of different size in CSF are a function of the steady state tissue concentration varying with varying CSF flow rate (Appendix). Thus "selectivity" is not changed in spite of mean CSF/serum quotients approaching each other with increasing protein concentration in CSF. This is consistent with the original observation of Schliep and Felgenhauer (1978). They have shown that the serum/CSF quotients of the large molecule α_2-macroglobulin and the smaller albumin approached each other with increasing CSF protein content but never reached the same values in spite of most severe blood-CSF barrier "breakdown".

I have to emphasize that these statements refer to the rate limiting step of the protein transfer from blood into CSF. There are morphological blood-brain barrier changes concomitant with neurological diseases (Bradbury 1979), but obviously these blood-brain barrier changes do not affect the rate limiting step for protein diffusion into CSF along the blood-CSF barrier: severe lesions of the blood brain barrier in multiple sclerosis, indicated by magnetic resonance imaging, do not correlate with the almost unchanged protein content in CSF (Felgenhauer and Reiber 1992).

Hyperbolic function and clinical application

The sensitive discrimination between a brain-derived protein fraction and a blood-derived fraction in CSF is of clinical relevance for detection of intrathecal immunoglobulin synthesis or specific antibody synthesis (Felgenhauer and Reiber 1992). Immunoglobulin CSF/serum quotient diagrams with reference to the albumin quotient are well established – but with different discrimination lines or formulas to detect the intrathecal protein synthesis.

The introduction of empirically formed hyperbolic discrimination lines (Reiber and Felgenhauer 1987) now find a theoretical confirmation. As mathematically derived from the laws of diffusion (Appendix), the ratio between two quotients (e.g. $Q_{IgG} : Q_{Alb}$) varies

according to a hyperbolic function. This aspect is independent of the statements about CSF flow.

Due to the larger number of cases in this study, the empirical fit of the hyperbolic function (especially the upper curves for discrimination between blood-derived and brain-derived CSF fractions) was improved in the range of small albumin quotients, compared with the earlier report (Reiber and Felgenhauer 1987). The higher sensitivity for pathological IgG, IgA and IgM quotients might be of clinical relevance, mainly for neuropediatric cases or ventricular CSF with smaller albumin quotients. It seems that with this improvement, the above theoretical foundation and the high clinical relevance (Souverijn et al. 1991) the quotient diagrams with a hyperbolic discrimination function, among the many approaches (Link and Tibbling 1977; Tourtellotte 1978; Reiber 1980; Thompson 1988; Öhman et al. 1992), could become the generally acceptable, physiologically correct basis for the graphical and numerical evaluation of serum proteins in CSF.

Physiological interpretations

Many unexplained facts from the physiology of CSF and pathophysiology of neurological diseases can be seen in a new light if the CSF flow model is applied.

The normal human newborn has extremely high CSF protein concentrations with Q_{Alb} values up to $30 \cdot 10^{-3}$ (Statz and Felgenhauer 1983). Earlier interpretations suggested an immature blood-CSF barrier with poor selectivity and high permeability. However, there is no doubt that early in gestation the anatomical structures for barriers are present (Mollgard and Saunders 1986). In the quotient diagrams there is no difference in selectivity, i.e. in molecular size-dependent discrimination by the blood-CSF barrier function for proteins in newborn children, when compared to mature adults with corresponding albumin quotients. The reported prenatal onset of CSF flow (Mollgard and Saunders 1986) must gradually reduce the protein concentration in CSF as the flow rate increases. It might be due to the late structural changes of the arachnoid villi and granulations (Upton and Weller 1985) which brings CSF drainage to a maximum about 4 months after birth with a minimum of Q_{Alb} at this time.

In the mature human a continuously increasing CSF protein concentration is observed. This age dependent increase could be explained by May et al. (1990) as a decrease in CSF production rate in elderly volunteers with a subsequently reduced CSF flow rate (0.4 ml/min in young to 0.19 ml/min in elderly volunteers).

For CNS leukemia, which is primarily an arachnoid disease with changes in trabeculae, a reduced CSF flow was suggested from histopathology (Price and Johnson 1973).

A purulent bacterial meningitis is accompanied by an increased CSF viscosity and meningeal adhesions. Protein complexes and cell deposits (Yamashima 1988) in the arachnoid villi have been detected in post mortem material. This again would be a severe handicap for CSF bulk flow.

Polyradiculitis of the type Guillain Barré may be accompanied by swelling in the region of the spinal roots (cauda equina) probably reducing flow through arachnoid villi into the veins associated with spinal nerve roots (Upton and Weller 1985).

In spinal blockade (Froin's syndrome), caudally to the blockade, high serum protein values are measured in lumbar CSF in spite of normal cisternal or ventricular CSF values (Davson 1967). In contrast to blood derived proteins, the brain derived proteins (prealbumin) have a decreased concentration relative to albumin caudal to a spinal blockade (Hill et al. 1959). In this case again the molecular size dependent discrimination (selectivity) for protein transfer between blood and CSF is not disturbed.

Ascorbate, a low molecular weight substance, is 6-fold increased in human lumbar CSF over blood concentrations due to an active transport through the choroid plexus. The decrease of ascorbate concentrations in the blood in cases of blood-CSF barrier dysfunction can be explained by the decreasing CSF flow rate (Reiber et al. 1993). This decrease of blood ascorbate concentration contradicts a barrier "leakage", by which an increased instead of a decreased ascorbate concentration in blood should be induced. This extraordinary example from a small molecule in the CSF offers a strong argument against changes in structures in case of blood-CSF barrier dysfunction.

A larger mean IgG-Index ($Q_{IgG}/Q_{Alb} = 0.8$) in smaller mammalian species (rats, guinea pigs (Suckling et al. 1986)) compared to 0.43 in humans (Reiber and Thiele 1983) can be explained partly by a shorter effective pathlength for protein diffusion from blood to CSF and mainly by a difference in CSF flow rate (Upton and Weller 1985) due to different CSF production rates (Davson 1967). There is no necessity to suggest a difference in selectivity of the barrier function. The increased CSF protein content in experimental allergic encephalomyelitis of the guinea pig (Suckling et al. 1986), regarded as model for multiple sclerosis, might be explained by its primarily spinal lesions, which is different from the disseminated process in multiple sclerosis with only minor changes in CSF protein content (Felgenhauer and Reiber 1992).

Finally, one could question whether the commonly used term "blood-CSF barrier dysfunction" functionally including CSF flow should be replaced by terms which describe the actually occurring "increased CSF protein content" as a "CSF flow reduction". At least the misleading terms blood-CSF barrier "impairment", "barrier breakdown", or "leakage" should be avoided.

A functional definition of the blood-CSF barrier is related to a varying CSF flow and subsequently varying protein gradients in the CNS tissue together with a varying molecular net flux for proteins. These aspects are common to normal blood-CSF barrier function and dysfunction, the latter characterized by a gradually decreasing CSF flow rate.

Appendix

Diffusion

The general law of diffusion (Fick's first law) is based on the following observation: The rate of transfer (n moles/s) of diffusing substance through unit area (1 cm^2) of a section is proportional to the concentration gradient measured normal to the section, i.e.

$$J = -D\frac{dc}{dx} \tag{1}$$

where c is the concentration of diffusing substance, x the space coordinate measured normal to the section, and D is called the diffusion coefficient.

The concentration gradient dc/dx is negative as its slope is negative in the direction of molecular flux (Fig. 5).

The fundamental differential equation of diffusion (Fick's second law of diffusion) is derived from (1) with the differential equation of continuity (van Holde 1971 or Crank 1975).

$$\frac{\partial c}{\partial t} = D\frac{\partial^2 c}{\partial x^2} \tag{2}$$

General solutions of the diffusion equation can be obtained for a variety of initial and boundary conditions provided the diffusion coefficient is constant (Crank 1975, Carslaw and Jaeger 1959). By differentiation of Eq. (3) we see that it is a basic solution of Eq. (2):

$$c = \frac{A}{t^{1/2}} e^{-x^2/4Dt} \tag{3}$$

where A is an arbitrary constant. This expression is symmetrical with respect to $x = 0$, tends to zero as x approaches infinity ($-\infty < x < \infty$) for $t > 0$ and for $t = 0$ it vanishes everywhere except at $x = 0$, where it becomes infinite. The concentration distribution has the shape of the Gaussian error curve (e.g. like $f'(x)$ in Fig. 6, not to be confused with the error function obtainded by the integration of the exponential). With a solution of the type in Eq. (3) it is possible to describe the case of a limited amount of substance diffusing in a cylinder of infinite length (column chromatography, van Holde 1971) or as the source solution to describe the release of a quantity of heat per unit area over the plane $x = 0$ at time $t = 0$ (Carslaw and Jaeger 1959, p. 50).

The case relevant for the diffusion through the blood-CSF barrier into flowing CSF (Fig. 7) has different boundary conditions which can be described as diffusion in a semi-infinite media with constant concentration c_0 at one surface ($x = 0$). This needs a treatment as extended initial distribution (integration of Eq. (3)) and a reflection at the boundary $x = 0$. According to Crank (1975, p. 14), we obtain

$$c_{x,t} = \frac{c_0}{2\sqrt{\pi Dt}} \int_x^\infty e^{-x^2/4Dt}\, dx$$

$$= \frac{c_0}{2\sqrt{\pi Dt}} \left(1 - \int_0^x e^{-x^2/4Dt}\, dx\right) \tag{4}$$

or

$$c_{x,t} = \frac{c_0}{\sqrt{\pi}} \int_z^\infty e^{-z^2}\, dz \tag{4b}$$

with $z = x/2\sqrt{Dt}$ and $dx = 2\sqrt{Dt}\, dz$

For conversion of these formulas it is important to know that $\int_{-\infty}^{\infty} e^{-z^2} dz = \sqrt{\pi}$ (Jost 1960, p. 27). The function of $c_{x,t}$ (Eqns. 4 and 4b) is shown in Fig. 6.

The Eq. (4) can be written as a standard mathematical function, the error function (erf z). The error function enters into the solution of a diffusion problem as a consequence of summing the effect of a series of line sources, each yielding an exponential type of distribution (Carslaw and Jaeger 1959, p. 482):

$$\operatorname{erf} z = \frac{2}{\sqrt{\pi}} \int_0^z e^{-z^2}\, dz \tag{4c}$$

and the error function complement

$$\operatorname{erfc} z = \frac{2}{\sqrt{\pi}} \int_z^\infty e^{-z^2}\, dz = 1 - \operatorname{erf} z \tag{4d}$$

For Eqn. 4 we find then (Crank 1975, p. 14)

$$Q = \frac{c_{x,t}}{c_0} = \frac{1}{2}\operatorname{erfc} z \tag{5}$$

Approximations for erf z are calculated for large and for small values of z from trigonometrical series type of solutions (Crank 1972, p. 21, and Carslaw and Jaeger 1959). We look at values of large z as $c_{x,t} \ll c_0/2$

TABLE 5

CONCENTRATION RATIOS ($Q_B:Q_A$) OF TWO DIFFUSANTS AT z_p (EFFECTIVE DIFFUSION PATH LENGTH)

Data for $Q_A = 1/2$ erfc z' and $Q_B = 1/2$ erfc z_p are calculated from the tables of Carslaw and Jaeger (1959, p. 482). The arbitrary ratio of diffusion constants $D_B:D_A = 1:2.25$ corresponds to $z':z_p = 1:1.5$ ($z' = z_p\,(D_B/D_A)^{1/2}$). Q_B(fit) represents the data calculated from Q_A with the hyperbolic function $Q_B = a/b\sqrt{Q_A^2 + b^2} - c$ for the fitted values $a = c = 0.8736$ and $b = 0.4087$. The comparison of the theoretical values Q_B with Q_B(fit) indicate that the ratio of $Q_B:Q_A$ with increasing Q_A follows a hyperbolic function.

Q_A		Q_B		Q_B(fit)
z'	1/2 erfc z	z_p	1/2 erfc z	
0.1	0.4438	0.15	0.4160	0.4160
0.2	0.3886	0.3	0.3356	0.3318
0.3	0.3356	0.45	0.2622	0.2567
0.4	0.2858	0.6	0.1980	0.1923
0.5	0.2397	0.75	0.1444	0.1391
0.6	0.1980	0.9	0.1015	0.0971
0.8	0.1289	1.2	0.0448	0.0424
1.0	0.0786	1.5	0.0169	0.0160
1.2	0.0448	1.8	0.00545	0.00524
1.4	0.0238	2.1	0.00148	0.00149

($Q = 0.5$). Therefore the error function complement becomes relevant:

$$\text{erfc } z = \frac{1}{\sqrt{\pi}} e^{-z^2}\left(\frac{1}{2} - \frac{1}{2z^3} + \frac{1\cdot 3}{2^2 z^5} - \frac{1\cdot 3\cdot 5}{2^3 z^7} + \dots\right) \tag{5b}$$

Values of this function are reported in tables (Carslaw and Jaeger 1959, p. 482), extracts of which are shown in Table 5.

Another important relation in diffusion is the mean displacement of diffusing particles which describes the shift of diffusing molecules in the matter depending on time and diffusion constant:

$$\bar{x} = \sqrt{2Dt} \tag{6}$$

where $\sqrt{Dt}$ represents a length (Jost 1960, p. 25).
$\bar{x}$ is comparable with the half width of the error curve. With increasing mean displacement (penetration depth), the maximal gradient dc/dx decreases (decreasing height, for dc/dx at $x_{0.5}$ in Fig. 6).

It is important to treat the system (Fig. 7) as a semi-infinite system and not as a plane sheet (slab) with two constant concentrations at both surfaces, i.e. with two reflection planes, and $dJ/dx = 0$ for $x = 0$ and $x = x_p$. This condition $dJ/dx = 0$ represents a linear concentration gradient, $(c_o - c_{CSF})/2$, with the consequences that the smaller molecule (albumin) with a smaller gradient dc/dx (also at x_p) would show the smaller molecular flux into CSF compared to the larger molecule (e.g. IgM), both decreasing with increasing CSF concentration. This is contradictory to the results in Table 4. Only in case of a nonlinear concentration gradient ($dJ/dx = dc/dt$) the smaller molecule A (Fig. 5) has a larger molecular flux into CSF,increasing with increasing CSF concentration.

CSF concentration gradient and blood-CSF barrier concentration gradient

Fig. 7 represents the terms used in the following equations for the CSF concentration gradient in subarachnoid space (y = direction of CSF flow) and the per-pendicular tissue concentration gradient (x = direction of molecular flux). The structural conditions are the same in the single person for the comparison of various plasma proteins in CSF so that the idealized conditions are valid for this comparison. For the concentration gradient along the neuraxis (y-direction) between the ventricles and lumbar subarachnoid space we find (with constant CSF flow rate):

$$c_{CSF}(y + \Delta y) = c_{CSF}(y) + \Delta c_{CSF} - \Delta c_{reflux} \tag{7}$$

The concentration, c_{CSF}, of a plasma protein species in CSF is increased along the interval Δy gradually by molecular flux into CSF (Δc_{CSF}) and is reduced to some extent by flux out of CSF (Δc_{reflux}) negligible under normal or moderate pathological conditions. Δc_{CSF} represents the local contribution of molecular flux from blood into CSF increasing along the neuraxis.

In a linear approach the molecular flux is characterized by J_i from Fick's first law of diffusion in Eqn. 1. According to Fig. 7 for a molecule i we get:

$$J_i = -D_i dc_i/dx = n_i/(\Delta t \cdot S) \tag{8}$$

n_i molecules passing the surfaces, S, of an interval of the subarachnoid space in time interval Δt into a volume ΔVol of CSF, flowing through this interval with constant rate, increase the CSF concentration according to Eqn. 9:

$$\Delta c_{iCSF} = n_i/\Delta \text{Vol}. \tag{9}$$

The bulk volume flow (F) of CSF (Fig. 7) is given in Eqn. 10:

$$F = \Delta \text{Vol}/\Delta t \tag{10}$$

This bulk volume flow (dimension ml/s) characterizes the volume ($\Delta \text{Vol} = A \cdot \Delta y$), which passes the cross section area A in the time interval Δt (Fig. 7). The flow rate of a single molecule in this CSF volume is $r = \Delta y/\Delta t$ (dimension cm/s) or $r = F/A$.

Eqns. 8 and 10 are solved for n_i and ΔVol respectively and these expressions are inserted into Eqn. 9 for the steady state. Additionally, we obtain with $F = r \cdot A$ (flow rate, r, times cross section area, A, shown in Fig. 7):

$$\Delta c_{iCSF} = \frac{J_i \cdot S}{F} = \frac{J_i}{r} \cdot \frac{S}{A} \tag{11}$$

The value S/A in the interval Δy (Fig. 7) is a constant (Const) for all proteins compared in the single patient. Thus Eqn. 11 represents the relation between local increase of CSF protein concentration, CSF flow rate and molecular flux:

$$\Delta\text{CSF protein concentration} = \frac{\text{molecular flux}}{\text{CSF flow rate}} \cdot \text{Const} \tag{12}$$

The linear form of Eqns. 11 and 12 find acceptance in the literature (Rapoport 1983). But, what has been overlooked so far is the fact that the molecular flux, $J_i \sim -dc/dx$, itself is a function of the CSF flow rate: With dc/dt and the differential equation of continuity (van Holde 1971) $dc/dt = -dJ/dx$, we get $dc/dt = Dd^2c/dx^2$ (Fick's second law of diffusion, Eqn. 2).

In case of the relevant nonlinear approach, $dc/dx = f'(x)$ is the derivative of Eqn. 4, shown in Fig. 6. This has two consequences: With increasing c_{CSF}, due to decreasing CSF flow rate, the local concentration gradient dc/dx (at x_p, in Fig. 5) increases! as long as $c_{CSF} < c_o/2$ or $Q < 0.5$ and decreases only for the rare case of quotients $Q > 0.5$ ($500 \cdot 10^{-3}$).

The second consequence is that with increasing c_{CSF} along the neuraxis (at constant CSF flow rate), the local concentration gradient increases too. The molecular flux into CSF increases nonlinearly with increasing distance from the ventricles. This is consistant with the report that labeled proteins from blood appear first in lumbar CSF and later in cisternal or ventricular CSF.

This nonlinear approach for Eqn. 11 represents the actual improvement of a mathematical description of the blood-CSF barrier function.

CSF flow rate

A decreasing flow rate, r, has a twofold influence on the CSF protein concentration: The volume, ΔVol, flowing through the interval Δy (Fig. 7) is reduced linearly with r, i.e. $\Delta Vol = r \cdot A \cdot t$ or $r \sim Vol/\Delta t$. As a consequence of decreasing ΔVol, Δc_{CSF} increases due to Eqn. 9 with decreasing CSF flow rate.

For the observed protein transfer from blood into CSF it is a reasonable postulate that under steady state conditions $c_{x,t}$ the local tissue concentration at the border with the subarachnoid space (Fig. 5) is equal to or larger than the CSF concentration c_{CSF}:

$$c_{x,t} \geq c_{CSF} \tag{13}$$

The reduced volume exchange rate with a subsequent increase in c_{CSF} induces an increased tissue concentration $c_{x,t}$ according to the condition of Eqn. 13.

This event is demonstrated in Fig. 5 as case two: the concentration curve B (e.g. IgG under steady state conditions) changes after the pathological event to curve A. With increasing concentration $c_{x,t}$ at x_p (Fig. 5) we get a larger mean displacement of particles (Eqn. 6): $\sqrt{D_B t}$ increases with time for constant D_B. It is a consequence of the nonlinear concentration gradient ($dc/dx = f'(x)$, with a maximum for $c = 0.5 \cdot c_o$ in Fig. 6), that with the increase of Q_B to Q_A the slope of the local gradient dc/dx increases. In this pathological case of decreasing r and increasing $c_{x,t}$, the molecular flux, J_i, increases without any change in the barrier structure. $J = f(1/r)$ leads to a nonlinear function of Δc_{CSF} in Eqs. 11 and 12. With Eqn. 8 we find that $n_i = f(1/r)$. From Eqn. 9 together with $\Delta Vol = f(r)$ we see immediately that, as a linearised approach,

$$c_{CSF} \sim 1/r^2 \text{ (for } Q \ll 0.5) \tag{14}$$

As an empirical approach the albumin quotient $\Delta Q_{Alb} = \Delta Q c_{CSF}/c_o$ can be used to characterize changes in CSF flow rate according to

$$r \sim 1/\sqrt{\Delta Q_{Alb}} \tag{15}$$

Hyperbolic function of quotient ratios

The ratio between CSF/serum concentration quotients of IgG, IgA or IgM and the albumin quotient (Figs. 1–3) is used for the discrimination of a blood derived protein fraction from a brain derived fraction in CSF (Reiber and Felgenhauer 1987). Amongst the many different approaches, the empirically fitted hyperbolic function is also a clinically confirmed "best fit" (Souverijn et al. 1991). Now the hyperbolic function can be derived theoretically from the diffusion Eqn. 2.

The relevant ratio of $Q_A : Q_B$ at x_p in Fig. 5 (explanation case 1) cannot be expressed in an explicit function from the general differential Eqn. 2 or Eqn. 4.

By projection of curve A onto curve B (Fig. 5), we get the concentration Q_A and Q_B on the same curve for different values of x (x′ and x_p, respectively).

This transformation of a curve A into curve B (Fig. 5) represents the approach of Carslaw and Jaeger (1959, p. 24) to introduce dimensionless parameters.

The position of a point x for the curve $c_{x,t}$ (Fig. 6 or Fig. 5) in the region $-l < x < +l$ can be specified by the position ratio x/l.

In fact, the only difference between the curve A and B is the mean displacement $\bar{x}_A = \sqrt{2D_A t}$ and $\bar{x}_B = \sqrt{2D_B t}$. The dimensionless position ratio is obtained by $x/\bar{x}$, i.e. the transfer of Q_A (on curve A at x_p) to curve B (Fig. 5) gives the same value Q_A at x′ on curve B if $x' = x_p \cdot \bar{x}_B/\bar{x}_A = x_p\ (D_B/D_A)^{1/2}$. D_A represents the diffusion constant of the smaller molecule A, i.e. $D_A > D_B$.

With this transform, we obtain the concentration ratio for two different distances x on the same curve with the identical error function ($z = x/2\sqrt{D_B t}$, see Eqn. (4b)). As a consequence of $Q_B : Q_A = \text{erfc } z_p$: erfc $z' = \text{erfc } z(D_B/D_A)^{1/2}$: erfc z, we get the general equation:

$$Q_B = \frac{\text{erfc } z(D_B/D_A)^{1/2}}{\text{erfc } z} \cdot Q_A \qquad (16)$$

It remains to show that this Eqn. 16 represents a hyperbolic function. The values of Q_B and Q_A calculated according Eqn. 5 with the tabulated values of erfc z (Carslaw and Jaeger 1959, p. 482) are shown in Table 5 for an arbitrary pair of molecules with the ratio of diffusion constants:

$$(D_B)^{1/2} : (D_A)^{1/2} = 1 : 1.5$$

The corresponding values of Q_B and Q_A fit the hyperbolic function

$$(y + c)^2/a^2 - x^2/b^2 = 1 \text{ or } Q_B = a/b\sqrt{Q_A^2 + b^2} - c.$$

Q_B(fit) shows the data calculated from Q_A with the fitted values a = c = 0.8736 and b = 0.4087. The excellent concordance of Q_B(fit) with the theoretical value of Q_B (Table 5) demonstrates that Eqn. 16 represents a hyperbolic function. This means that the concentration ratio of molecules of different size diffusing through the same matter (e.g. plane sheet, slab) with a constant ratio of their diffusion coefficients is generally characterized by a hyperbolic function. The shape of this hyperbolic curve is determined only by the ratio of the square roots of both diffusion coefficients (Eqn. 16).

Acknowledgements I thank Prof. K. Felgenhauer, Göttingen, Prof. S.I. Rapoport, Bethesda, and especially Prof. E.J. Thompson, London, together with an unknown referee, for critical comments, improving the argumentation and presentation.

References

Bradbury, M. (1979) The Concept of a Blood-Brain Barrier, John Wiley and Sons, Chichester.

Carslaw, H.S. and Jaeger, J.C. (1959) Conduction of heat in solids. Clarendon Press, Oxford, 2nd ed.

Cestan, Laborde and Riser (1925) La perméabilité meningée n'est qu'un des modes de la perméabilité vasculaire. Pr. méd. 33: 1330–1332.

Crank, J. (1975) The Mathematics of Diffusion, Clarendon Press, Oxford, 2nd edn.

Cutler, R.W.P., Deuel, R.K. and Barlow, Ch.F. (1967) Albumin exchange between Plasma and CSF. Arch. Neurol., 17: 261–270 and 17: 620–628.

Davson, H. (1967) Physiology of the Cerebrospinal Fluid, Churchill, London.

Davson, H., Welch K. and Segal, M.B. (1987) Physiology and Pathophysiology of the Cerebrospinal Fluid, Churchill, London.

Felgenhauer, K. (1974) Protein size and cerebrospinal fluid composition. Klin. Wschr., 52: 1158–1164.

Felgenhauer, K. and Reiber, H. (1992) The diagnostic significance of antibody specificity indices in multiple sclerosis and herpes virus induced diseases of the nervous system. Clin. Invest., 70: 28–37.

Frick, E. and Scheid-Seydel, L. (1958) Untersuchungen mit I131-markiertem Albumin über Austauschvorgänge zwischen Plasma und Liquor cerebrospinalis. Klin. Wschr., 36: 66–69 and 36: 857–863.

Hill, N.C., Goldstein, N.P., Mc Kenzie, B.F., Mc Guchin, W.F. and Sviers, H.J. (1959) Cerebrospinal fluid proteins, glycoproteins and lipoproteins in obstructive lesions of the central nervous system. Brain, 82: 581–593.

Jost, W. (1960) Diffusion in Solids, Liquids, Gases, Academic Press, New York, 3rd edn.

Link, H., Tibbling, G. (1977) Principles of albumin and IgG disorders. Evaluation of IgG synthesis within the central nervous system in multiple sclerosis. Scand. J. Clin. Lab. Invest., 37: 397–401.

May, C., Kaye, J.A., Atack, J.R., Schapiro, M.B., Friedland, R.P. and Rapoport, S.I. (1990) Cerebrospinal fluid production is reduced in healthy aging. Neurol., 40: 500–503.

Mollgard, K. and Saunders, N.R. (1986) The development of the human blood-brain and blood-CSF barriers. Neuropath. Appl. Neurobiol., 12: 337–358

Öhman, S., Ernerudh, J., Forsberg, P., Henriksson, A., von Schenck, H. and Vrethem, M. (1992) Comparison of seven formulas and isoelectrofocusing for determination of intrathecally produced IgG in neurological diseases. Ann. Clin. Biochem., 29: 405–410.

Ogston, A.F. (1956) Sedimentation, diffusion and viscosity. In: Physical Techniques in Biological Research, Academic Press, New York, pp. 137–138.

Price, R.A. and Johnson, W.W. (1973) The central nervous system in childhood leukemia. I. The arachnoid. Cancer, 31: 520–523.

Rapoport, S.I. (1983) Passage of proteins from blood to cerebrospinal fluid. In: Wood, J.H. (Ed.), Neurobiology of Cerebrospinal Fluid, Vol. 2, Plenum Press, New York, pp. 233–245.

Reiber, H. (1980) The discrimination between different blood-CSF barrier dysfunctions and inflammatory reactions of the CNS by a recent evaluation graph for the protein profile of CSF.J. Neurol., 224: 89–99.

Reiber, H. (1986) Evaluation of blood-cerebrospinal fluid barrier dysfunctions in neurological diseases. In: Suckling, A.J., Rumsby, M.G. and Bradbury, M.W.B. (Eds.), The Blood-Brain Barrier in Health and Disease, Ellis Horwood, Chichester, pp. 147–157.

Reiber, H. (1993) Decreased Flow of Cerebrospinal Fluid (CSF) as Origin of the Pathological Increase of Protein Concentration in CSF. In: Felgenhauer, K., Holzgraefe, M. and Prange, H. (Eds.), CNS Barriers and Modern CSF Diagnostics, Verlag Chemie, Weinheim, pp. 305–317.

Reiber, H. and Felgenhauer, K. (1987) Protein transfer at the blood cerebrospinal fluid barrier and the quantitation of the humoral immune response within the central nervous system. Clin. Chim. Acta, 163: 319–328.

Reiber, H. and Thiele, P. (1983) Species-dependent variables in blood cerebrospinal fluid barrier function for proteins. J. Clin. Chem. Clin. Biochem., 21: 199–202.

Reiber, H., Ruff, M. and Uhr, M. (1993) Ascorbate concentration in human cerebrospinal fluid (CSF) and serum. Intrathecal accumulation and CSF flow rate. Clin. Chim. Acta, in press.

Schliep, G. and Felgenhauer, K. (1978) Serum-CSF protein gradients, the blood CSF barrier and the local immune response. J. Neurol., 218: 77–96.

Souverijn, J.H.M., Serrée, H.M.P., Peet, R., Grenzebach Smit, W. and Bruyn, G.W. (1991) Intrathecal immunoglobulin synthesis. Comparison of various formulae with the "gold standard" of isoelectric focussing. J. Neurol. Sci., 102: 11–16.

Statz, A. and Felgenhauer, K. (1983) Development of blood-CSF barrier. Dev. Med. Child. Neurol., 25: 152–161.

Suckling, A.J., Reiber, H. and Rumsby, M.G. (1986) The blood-CSF barrier in chronic relapsing experimental allergic encephalomyelitis. In: Suckling, A.J., Rumsby, M.G. and Bradbury, M.W.B. (Eds.), The Blood-Brain Barrier in Health and Disease. Ellis Horwood, Chichester, pp. 147–157.

Thompson, E.J. (1988) The CSF Proteins: A Biochemical Approach. Elsevier, Amsterdam.

Tourtellotte, W.W. and Ma, B.J. (1978) Multiple sclerosis: the blood-brain barrier and the measurement of the de novo central nervous system IgG synthesis. Neurology, 28: 76–83.

Upton, M.L. and Weller, R.O. (1985) The morphology of cerebrospinal fluid drainage pathways in human arachnoid granulations. J. Neurosurg., 63: 867–875.

Van Holde, K.E. (1971) Physical Biochemistry. Prentice Hall Int., Englewood Cliffs, NJ.

Yamashima, T. (1988) Functional ultrastructure of cerebrospinal fluid drainage channels in human arachnoid villi. J. Neurosurg., 22: 633–641.